

Ultrathin AlN/GaN Heterojunctions by MBE for THz Applications

Yu Cao and Debdeep Jena

Electrical Engineering, University of Notre Dame, Notre Dame, IN, 46556

ABSTRACT

High electron mobility transistors (HEMTs) based on all-binary AlN/GaN heterostructures are attractive candidates for the generation and detection of terahertz (THz) radiation. The basic requirements are that a) the electron density in the 2DEG should be large enough for ensuring that the electron-electron scattering mean-free path is much shorter than the distance between the contacts to ensure a viscous, fluid-like flow, and b) the mobility should be high enough such that the possible plasma modes are not strongly damped. In comparison to other semiconductors, the large spontaneous and piezoelectric polarization difference between coherently strained ultrathin AlN layers grown on GaN can achieve 2DEG densities exceeding $3 \times 10^{13} \text{ cm}^{-2}$, and possibly approaching values as high as $6 \times 10^{13} \text{ cm}^{-2}$. The plasma frequencies achievable in such extremely high density 2DEGs are higher than HEMTs based on other material systems. The absence of alloy scattering in these all-binary heterojunctions allows for high mobilities as well, as is demonstrated in this work by RF MBE growth; this is critical for sustaining plasma oscillations.

INTRODUCTION

In 1970, terahertz electromagnetic radiation was observed from a LiNbO₃ crystal under picosecond-pulsed optical excitation [1]. Since then, a lot of research has been done to generate THz radiation using either picosecond or femtosecond optical pulses incident upon various materials such as LiNbO₃, ZnTe, GaAs, InAs etc [2-6]. In 2002, Köhler *et al* demonstrated a GaAs-based electrically pumped quantum cascade laser operating at low temperatures for the generation of monochromatic 4.4 THz radiation [7]. This structure was further developed and more frequencies have been achieved [8, 9].

For all-electrical devices, Dyakanov and Shur proposed that both gated and ungated 2D electron gases satisfying certain boundary criteria can be used for generating terahertz radiation [10, 11]. Knap *et al* studied HEMTs based on InGaAs and AlGaIn/GaN heterostructures, and demonstrated voltage-tunable emission from 0.4 to 5 THz [12-14]. Dyakanov and Shur have predicted [11] that the electromagnetic radiation frequency f_0^{2D} is dependent on the square root of sheet carrier density n_s . Radiation from 2DEGs with low n_s has been studied in GaAs and InGaAs systems, which give f_0^{2D} less than 10 THz. A high 2DEG density with high electron mobility is necessary for generating higher frequencies. The widest range for n_s among semiconductors is in the III-V nitride semiconductors. Since 2DEGs in nitride HEMTs are generated by spontaneous and piezoelectric polarization, the highest 2DEG density possible is in an AlN/GaN heterostructure. In this report, the MBE growth, the structural and the transport properties of ultrathin AlN/GaN heterojunctions with very high n_s ($\sim 3 \times 10^{13} \text{ cm}^{-2}$) are described and shown to be attractive for THz devices based on plasma-wave instabilities.

THEORY

The plasma frequency in a general 2D electron system is given by

$$f_{2D} = \frac{1}{2\pi} \sqrt{\frac{e^2 n_s k}{2\epsilon_0 \epsilon_\infty m^*}}, \quad (1)$$

where e is the electron charge, n_s is the electron sheet density in the 2DEG, ϵ_0 is the permittivity of vacuum, ϵ_∞ is the high-frequency relative dielectric constant of the semiconductor, m^* is the electron effective mass, and k is a specific wave vector. The value of k depends on the geometry of the 2DEG and the boundary conditions. Dyakanov and Shur derived in 2005 that for an *ungated* 2DEG, $k = \frac{\pi 2l - 1}{2L}$ if the source is grounded and the drain is open, where L is the distance between the source and drain and l is an integer standing for the mode index [11]. In an earlier paper, they predicted THz emission from a gated structure with different boundary conditions [12]. For an estimate of the frequency of radiation, we use the Fermi vector $k_F = \sqrt{2\pi n_s}$ here. The fundamental 2DEG plasma frequency calculated for Si, GaAs, GaN, AlN and InAs is shown in Figure 1 (a). The 2D plasma frequency in all of these materials is in the THz regime. However, to sustain plasma oscillations for a reasonably large number of periods, the plasma frequency and momentum scattering time product should be much larger than 1. The product versus mobility for 2DEGs in AlGaAs/GaAs is plotted in Figure 1 (b), and compared with the corresponding product for an AlN/GaN heterojunction shown in Figure 1 (c). As is evident, from the three figures, AlN/GaN heterojunctions with very high 2DEG sheet densities are very attractive candidates for plasma-instability based THz generation. Though 2DEG densities of $\sim 6 \times 10^{13} \text{ cm}^{-2}$ are theoretically possible, they have not been demonstrated yet. Here we demonstrate 2DEGs in ultrashallow AlN/GaN heterojunctions with $n_s \geq 3 \times 10^{13} \text{ cm}^{-2}$, which are very attractive candidate for THz devices.

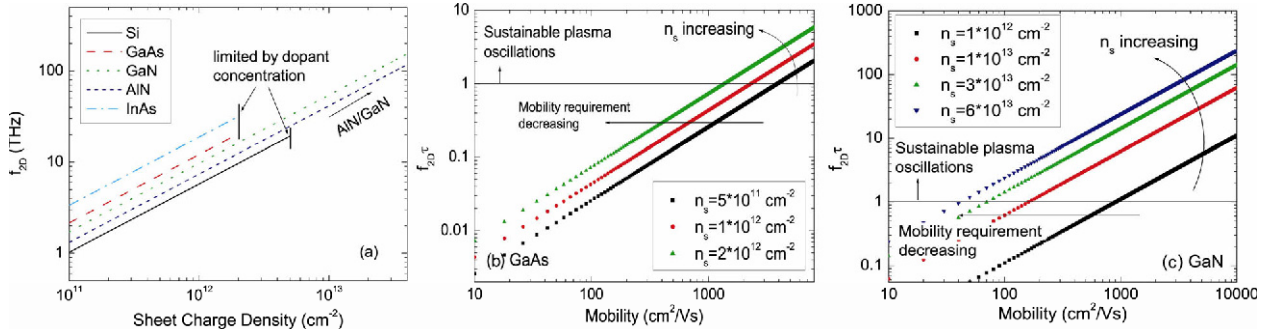


Figure 1 (a) the calculated 2D plasma frequency for Si, GaAs, GaN, AlN and InAs for different 2DEG densities, (b) product of the plasma frequency and momentum relaxation time for the 2DEG in AlGaAs/GaAs heterojunctions, and (c) same for 2DEGs in AlN/GaN heterojunctions.

EXPERIMENT

A series of AlN/GaN samples were grown by N_2 -source radio-frequency molecular-beam epitaxy (RFMBE) with different substrate temperatures at a RF plasma power of 275 W (growth rate: 216 nm/hr). The fluxes of Ga and Al were fixed at 1.56×10^{-7} Torr and 1.48×10^{-7} Torr respectively, and the substrate temperature was varied from 730-800° C. 3nm AlN layers

were grown on an undoped GaN layer, starting from a semi-insulating GaN substrate. The band diagram of the heterostructure is shown in Figure 2 (a), along with the calculated 2DEG spatial distribution. The structural and electronic transport properties of the ultrathin AlN/GaN structures were studied. AFM measurements showed smooth surface morphologies with atomic steps and dislocation terminations, with the surface roughness RMS in the 0.5 nm range for $2 \times 2 \mu\text{m}$ scan as shown in Figure 2 (b). Hall mobilities of $\sim 530 \text{ cm}^2/\text{V}\cdot\text{s}$ (room temperature) and $\sim 860 \text{ cm}^2/\text{V}\cdot\text{s}$ (77K), and 2DEG sheet carrier concentration of $\sim 2.5 \times 10^{13} \text{ cm}^{-2}$ were achieved. The 2DEG is located only $\sim 4 \text{ nm}$ below the sample surface and the transport properties show a marked improvement with an increasing growth temperature and lower growth rates. By growing a series of samples with different AlN thicknesses, the critical thickness was found to be between 4 nm and 5 nm. The maximum 2DEG density that was observed was $\sim 3.5 \times 10^{13} \text{ cm}^{-2}$. When the AlN layer was 5nm, cracks were observed on the surface along the hexagonal lattice of the underlying wurtzite GaN crystal as shown in Figure 2 (c). These cracks were observed to originate from the tips of the spiral hillocks at the tips of dislocations. The relaxation occurs at those points since the growth rate is larger at the tips of the dislocations.

Interestingly, due to the large spontaneous and piezoelectric polarization fields in the nitrides, one is not limited to just one 2DEG. Multiple parallel 2DEGs can be created at on AlN/GaN MQW structure. A $9 \times (\text{AlN}_{4.6\text{nm}}/\text{GaN}_{56\text{nm}})$ multiple quantum-well sample was also grown by RFMBE under slower growth conditions. The total sheet density in this sample was measured to be $\sim 8 \times 10^{13} \text{ cm}^{-2}$ with a 300 K mobility $\sim 1080 \text{ cm}^2/\text{V}\cdot\text{s}$. This clearly indicates the formation of multiple parallel 2DEGs with a high mobility, even at room-temperature. Such parallel 2DEGs are extremely attractive for the generation and detection of very high-frequency THz radiation, going well into the 100 THz range, and they should be usable at RT according to Figure 1(c).

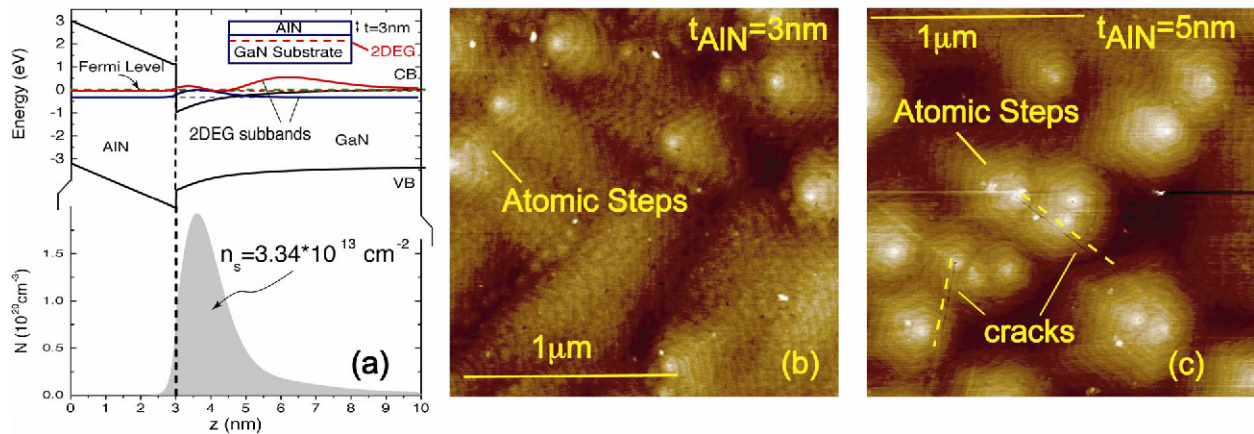


Figure 2 (a) Band diagram of AlN/GaN heterojunction & electron distribution along the growth direction, AFM images for (b) 3nm-thick AlN and (c) 5nm-thick AlN, showing that AlN remains coherently strained till $\sim 4 \text{ nm}$ thickness, resulting in $n_s \sim 3.10^{13}/\text{cm}^2$.

DISCUSSION & CONCLUSION

Since the plasma frequency increases with the 2DEG density, an all-binary AlN/GaN heterojunction offer an attractive route to the generation of high-frequency THz radiation. The absence of alloy scattering in these binary heterojunctions results in high mobilities, coupled with the very high electron densities achievable provides a motivation for studying the growth

and transport properties of ultrathin AlN/GaN heterojunctions. In addition, the location of the 2DEG very close to the sample surface will possibly enhance the emission by reducing losses incurred by free-carrier and defect-related absorption in the barrier layer. In principle, such ultrashallow 2DEGs at AlN/GaN heterojunctions are similar to surface accumulation/inversion layers in InAs & InN, which have been demonstrated to be sources of THz radiation. The plasma frequency achievable in the AlN/GaN heterostructures can reach ~100 THz for 2DEG densities $\sim 3.5 \times 10^{13} \text{ cm}^{-2}$, relaxing the requirements on the transport properties (mobility of $\sim 1000 \text{ cm}^2/\text{Vs}$ is needed, which is readily achievable at room temperature as demonstrated here). The extremely large range of 2DEG densities achievable by gate tuning and the electronic polarization in the material system makes the III-V Nitrides, and specifically AlN/GaN heterojunctions one of the most attractive systems for high-frequency THz radiation and detection.

REFERENCES

1. T. Yajima and N. Takeuchi, *Jpn. J. Appl. Phys.* **9**, 1361 (1970).
2. K. Yang, P. Richards and Y. Shen, *Appl. Phys. Lett.* **19**, 320 (1971).
3. L. Xu, X. Zhang and D. Auston, *Appl. Phys. Lett.* **61**, 1784 (1992).
4. M. Suzuki, T. Kiwa, M. Tonouchi, Y. Nakajima, S. Sasa and M. Inoue, *Phys. E* **22**, 574 (2004).
5. F. Teppe, D. Veksler, X. Xie, X. Zhang, S. Rumyantsev, W. Knap and M. Shur, *Appl. Phys. Lett.* **87**, 022102 (2005).
6. K. Vodopyanov, M. Fejer, X. Yu, J. Harris, Y. Lee, W. Hurlbut, V. Kozlov, D. Bliss and C. Lynch, *Appl. Phys. Lett.* **89**, 141119 (2006)
7. R. Köhler, A. Tredicucci, F. Beltram, H. Beere, E. Linfield, A. Davies, D. Ritchie, R. Lotti and F. Rossi, *Nature* **417**, 156 (2002).
8. S. Kumar, B. Williams and Q. Hu, *Appl. Phys. Lett.* **88**, 121123 (2006).
9. M. Vitiello and G. Scamarcio, *Appl. Phys. Lett.* **89**, 131114 (2006).
10. M. Dyakonov and M. Shur, *Phys. Rev. Lett.* **71**, 2465 (1993).
11. M. Dyakonov and M. Shur, *Appl. Phys. Lett.* **87**, 111501 (2005)
12. W. Knap, J. Lusakowski, T. Parenty, S. Bollaert, a. Cappy, V. Popov, M. Shur, *Appl. Phys. Lett.* **84**, 2331 (2004).
13. J. Lusakowski, W. Knap, N. Dyakonova, L. Varani, J. Mateos, T. Gonzalez, Y. Roelens, S. Bollaert, A. Cappy and K. Karpierz, *J. Appl. Phys.* **97**, 064307 (2005).
14. N. Dyakonova, A. Fatimy, J. Lusakowski, W. Knap, M. Dyakonov, M. Poisson, E. Morvan, S. Bollaert, A. Shchepetov, Y. Roelens, C. Gaquiere, D. Theron and A. Cappy, *Appl. Phys.* **88**, 141906 (2006)
15. S. Binari, K. Doverspike, G. Kelner, H. Dietrich and a. Wickenden, *Solid-State Electron.* **41**, 177 (1997).
16. E. Alekseev, A. Eisenbach, and d. Pavlidis, *Electron. Lett.* **35**, 2145 (1999).
17. I. Smorchkova, S. Keller, S. Heikman, C. Elsass, B. Heying, P. Fini, J. Speck and U. Mishra, *Appl. Phys. Lett.* **77**, 3998 (2000).